MOTION ESTIMATION OF A HAND-HELD MINE DETECTOR

Charles Beumier, Pascal Druyts, Yann Yvinec, Marc Acheroy

Royal Military Academy, Dept. of Elec. Engineering, SIC
Avenue de la Renaissance, 30, 1000 Bruxelles, Belgium
beumier,pascal.druyts,yvinec,acheroy@elec.rma.ac.be

ABSTRACT

This paper presents the results of simulating position estimation from a camera-based system integrated in a hand-held mine detector. The system reports positions of the sensor head relative to a bar placed on the ground by the deminer to indicate the safe limit. Monitoring the position during sensor scanning enables image reconstruction of the captured signals. Image representation allows object shape analysis and easy target localization. The simulation has considered several configurations including one or two cameras, one or no accelerometer and a 1 or 2-dimensional reference lattice on the bar. The required accuracy of the positioning system in our application is +/- 0.5 cm in each direction.

1. INTRODUCTION

Humanitarian mine clearance has recently received much attention in order to decrease the nuisance of infected regions [3]. Better clearance can be achieved by enhancing the classical metal detector with additional sensors to address the issues of false alarm reduction and plastic mine detection [2].
The European project HOPE (Hand-held OPErational demining system, [5]) aims at developing and building an efficient hand-held demining tool based on a metal detector (MD), a ground penetrating radar (GPR, indicating metallic and dielectric objects) and a microwave radiometer (MWR, indicating flushed objects). Higher detection rates and lower false alarms are expected from the combination of these sensors.
Imaging capabilities will be added to the system (3D for the GPR, 2D for the MD and the MWR) to increase false alarm discrimination by shape analysis [6] of detected objects. The advantage of image analysis has already been shown [7, 9]. Because we are concerned with a hand-held (as opposed to robotic [4]) detector, the sensor head position monotoring is not trivial. The project HOPE aims at estimating the position with an accuracy of +/- 0.5 cm in each direction.

2. DEMINING PROCEDURE

To make understand better the different possibilities we considered in the simulations, we present in this section a typical way to clear a minefield.
The field is divided into 1-meter wide lanes. These are cleared in parallel by the following procedure. First, a marker bar (100x2x2 cm) is laid on the ground to clearly show the limit of the 'Safe Area' (see Fig. 1). The deminer will never step over this bar. Secondly, the 'Search Area' (typically, 1 x 0.5 m) is cleared from disturbing objects or vegetation laying on the surface. The search area, delimited by a second bar, is scanned with the metal detector

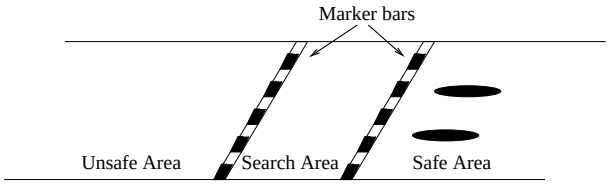

Figure 1: Use of marker bars in a typical demining procedure

and suspected spots are marked. These are later precisely localized and suspected objects are carefully extracted. Finally, when the search area has become a safe area, the bar is moved just before the 'Unsafe Area' and a new search is started.
We are aware that other (often similar) operational procedures are used by other demining teams. However, the one presented here is realistic and allows us to take profit from the existence of marker bars as localization reference and from the fact that limited areas (1 m by 0.5 m) are considered for each search area. These conditions, to be met with little effort by demining teams, made us think about using cameras to track the sensor head motion during scanning.

3. POSITION MONITORING SYSTEM

The first solution envisaged in HOPE concerns a gyroscopic positioning system [8]. Considering cost, bulkiness and weight criteria, the project also investigated an optical solution based on one or two cameras fixed on the detector stick (the hand-held mine detector).
The marker bars advantageously provide positioning references. First, their visibility is maximized from their location close to the search area. Secondly, they can easily contain a barcode with highly visible transitions providing for easily detected points. Finally, the barcode allows for point labelling, in each image independently, which simplifies the matching of points in a multiple-image approach.
Unfortunately, a rotation around the marker bar is hardly captured by a system relying on only one 1-Dimensional bar. To solve this problem, several solutions were considered.
First, an accelerometer can be used to sense inclination from the vertical direction (Fig. 2). The complication comes from the necessity to compensate for the acceleration due to the movement (and not due to gravity). For the sake of precision, a second camera may be added.
Secondly, the two marker bars delimiting the search area can be tracked. To maximize the visibility of the bars, it is preferable to

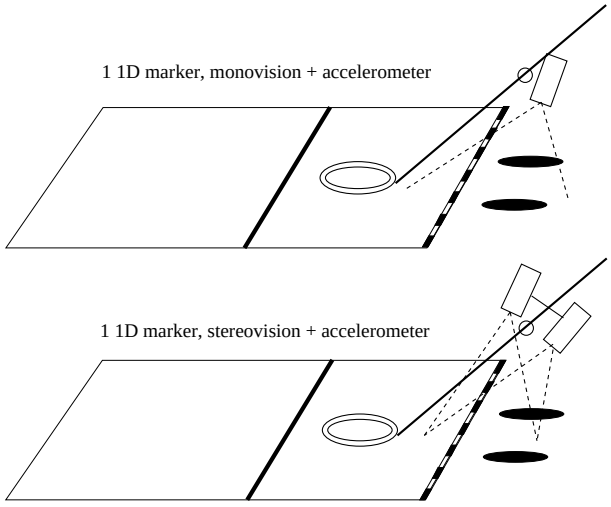

Figure 2: Systems with an accelerometer

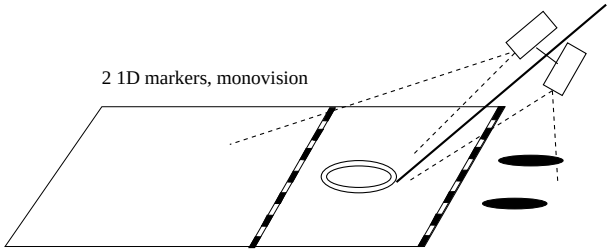

Figure 3: System tracking two marker bars

image each bar by its own camera (Fig. 3).

Thirdly, a 2-Dimensional lattice suffices to offer a reference for 3-D localization (see Fig. 4). The main disadvantage of this solution is to require a rather cumbersome marker bar. This approach was evaluated by another team (BATS, Belgium) and with a different scheme. It appeared that the error levels are higher, probably because of the limited extension of the lattice in one of the two dimensions.

To estimate the precision a positioning system can achieve, one has to describe a realistic movement (section 4), evaluate the parameters linked to the camera (section 5) and accelerometer and estimate the different non negligible levels of error (section 7).

4. MOVEMENT SIMULATION

For the simulation, a realistic scanning movement of the mine detector has been defined. It consists of the superposition of a lateral sweep and a forward progression (see Fig. 5).

From this movement and its dynamic, the position and angle of the camera and its acceleration are known at the different moments. This is necessary to extract the component due to the gravity from the accelerometer, which enables the measurement of the angle with the vertical.

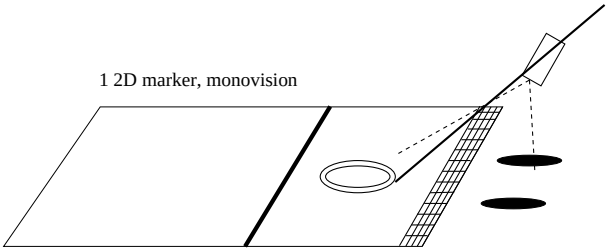

Figure 4: System with a 2-D marker

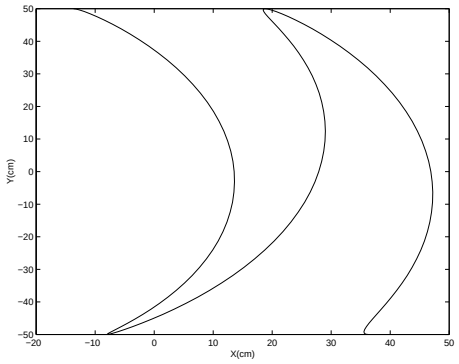

Figure 5: Simulated movement of the camera

5. CAMERA MODELIZATION

The values of the camera parameters are:

- CCD size: 1/4 inch
- Resolution: 768 x 576 pixels
- Pixel size in both directions: 8.3mm.

Due to the rather short distance of work (the cameras hang at about 60 to 100 cm above the ground level) and the rather large scanning zone (typically 100 cm x 50 cm), a short focal length (4mm) was necessary for the cameras. The induced non-linearity and distortion [1] are compensated by offset values (look-up table and interpolation) obtained during a calibration phase measuring the deformation encountered by a reference grid.

Fig. 6 top left shows an image of a grid used as reference. The nodes of the grid are localized as the intersections of horizontal and vertical lines obtained by following dark segments (Fig. 6 top right). The bottom images of the same figure show a capture of a grid at another distance and the compensation of the distortion thanks to the reference image (top left).

6. POSITION ESTIMATION

The position of the sensor head of the mine detector in the coordinate system linked to the marker bar (xyz) is derived from the position relative to the the camera axis system ($x_c y_c z_c$) by the relation

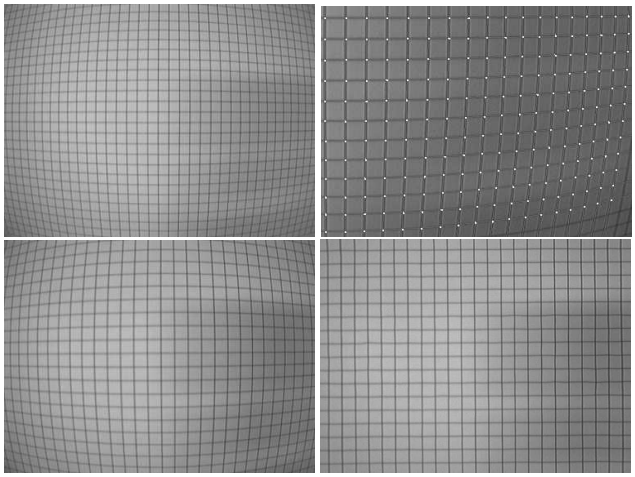

Figure 6: Distortion compensation: a) Reference image with grid. b) Close-up of image a with localized grid nodes. c) Another image of the grid. d) Compensation of image c according to the deformation measured in image a.

$$\begin{pmatrix} x_c \\ y_c \\ z_c \end{pmatrix} = R \times \begin{pmatrix} x \\ y \\ z \end{pmatrix} + T \qquad (1)$$

where R and T, respectively the rotation matrix and the translation vector, are supposed to be constant (the camera and the sensor head keep the same relative position).
Considering the pinhole model for the camera, image positions (x_i, y_i) are related to camera axis coordinates by

$$\begin{pmatrix} x_i \\ y_i \end{pmatrix} = \begin{pmatrix} f_{ex} \cdot \frac{x_c}{z_c} \\ f_{ey} \cdot \frac{y_c}{z_c} \end{pmatrix} \qquad (2)$$

where f_{ex}, f_{ey} are the focal length divided by the pixel dimension, repectively in the x and y directions.
For each reference point of the marker bar (along the Y axis: $\begin{pmatrix} x \\ y \\ z \end{pmatrix} = \begin{pmatrix} 0 \\ \alpha \\ 0 \end{pmatrix}$), equations (1) and (2) lead,

with $R = \left(1\vec{x}\,1\vec{y}\,1\vec{z}\right)$, $1\vec{y} = \begin{pmatrix} \theta_1 \\ \theta_2 \\ \theta_3 \end{pmatrix}$ and $T = \begin{pmatrix} \theta_4 \\ \theta_5 \\ \theta_6 \end{pmatrix}$, to:

$$\begin{cases} x_i \cdot (\alpha \cdot \theta_3 + \theta_6) = f_{ex} \cdot (\alpha \cdot \theta_1 + \theta_4) \\ y_i \cdot (\alpha \cdot \theta_3 + \theta_6) = f_{ey} \cdot (\alpha \cdot \theta_2 + \theta_5) \end{cases} \qquad (3)$$

The rather high number of reference points leads to an overdetermined system in the variables θ_i. Because the solution is independent of a multiplicative factor, we divide all the θ by $\frac{\theta_6}{\lambda}$, knowing that θ_6 is not 0 (the camera would then have its focal plane on the marker bar). We obtain $\theta = \lambda\,(\theta'_1, \theta'_2, \theta'_3, \theta'_4, \theta'_5, 1)$, with λ chosen so that the constraint $\theta_1^2 + \theta_2^2 + \theta_3^2 = 1$ holds.
Once the θ_i are identified, $1\vec{y}$ is known. A second direction such as the vertical (from the accelerometer) or the direction linking the centres of the 2 1D markers will define a perpendicular direction (by vector product) which is the second direction of the axis system. The third axis is obtained by vector product to form an orthogonal axis system. The naming convention of the coordinates is that Y is oriented along the bar, X in the direction of progression and Z more or less vertically (strictly vertical if an accelerometer is used).

7. ERRORS CONSIDERED IN THE SIMULATIONS

7.1. Camera parameters

The localization of the principal point (intersection of the optical axis with the image plane) is assumed to have an error of 1 pixel in both image directions. The ratios f_{ex} and f_{ey} are supposed to be estimated with an error of 1%. The distortion induced by the small focal length is supposed to be corrected up to a maximum of 2 pixels of error in both image directions.

7.2. Localization of marker points

The marker bar will consist of dark rectangles on a white background [10] and will provide for 100 reference corners situated on a line. For the simulation, their localization error was modelled by a random uniform distribution in the interval [-1..1] pixels. Also, the number of reference points were limited to the ones in the field of view of the camera.

7.3. Accelerometer

To model the measurement error of the accelerometer, we considered a Gaussian distribution with standard deviation of 5 thousandths of G. This value corresponds to the error level for a bandwidth of sollicitations slightly larger than $10Hz$.

8. SIMULATION RESULTS

The different solutions were simulated to have an estimate of the error levels and check the influence of specific causes.
Fig. 7 represents the position errors in each direction along the scan path as a result of the different error levels introduced in section 7.
This figure, similar for the different systems based on a 1-D marker bar, suggests that the position errors have an important bias, which can be eliminated by an appropriate calibration. It also shows that the error along Z is by far the most important, which is particularly true for the configurations involving an accelerometer which introduces an important incertitude in the Z direction. This observation is corroborated by the fact that the Z error is more important at the end of the scan, when the distance to the marker bar is larger.
We also noticed in the simulations some positions of the scan where the errors are higher. These correspond to the extremities of the sweep, where fewer marker points are visible from the camera. However, with a better positioning of the camera and a density of one marker per centimeter, the number of visible points seems sufficient to obtain the desired accuracy.
The level of errors in the three directions is summarized in Table 1 for standard deviation errors and Table 2 for peak to peak errors.
The error level in each direction meets the requirement of a +/- 0.5 cm of accuracy, except for the third option which could probably lead to better results since the second camera was not correctly oriented and sometimes saw few markers.

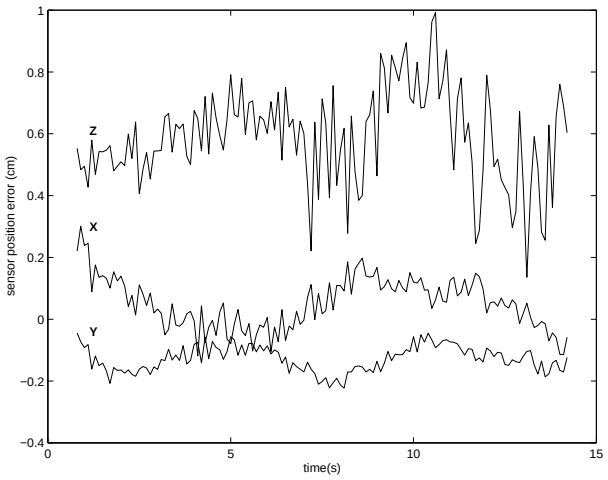

Figure 7: Position error in each direction as a result of all considered errors

Configuration	X (cm)	Y (cm)	Z (cm)
1)Mono, 1 marker	0.08	0.04	0.15
2)Stereo, 1 marker	0.08	0.04	0.13
3)Mono, 2 markers	0.09	0.04	0.14

Table 1: Standard deviation errors

9. CONCLUSIONS

Different configurations for position monitoring of a hand-held mine detector have been considered. They are based on one or two cameras and exploit the availability of one or two marker bars laid on the ground in normal demining practice. The current study analysed the position accuracy one can expect from the different sources of errors that such systems encounter.

The one camera approach benefits from simple acquisition hardware and problem solving. However, some incertitude remains concerning the precision of the accelerometer, such as, for instance, the possibility to correctly compensate for the acceleration due to the movement.

The two-camera solution did not seem to bring a sufficient increase in accuracy for the additional hardware and numerical complexity (parameter optimization with non-linear constraint) when compared with the first solution.

The use of the two marker bars could lead to the best accuracy if the second camera was better placed to see more markers. This solution is a good alternative to the first solution if the accelerometer brings problems.

Finally the method based on a 2-D marker has been evaluated by another research team and with a different approach. It appears however that the error levels are higher.

Acknowledgments

This project has been supported by the European ESPRIT project (EP 29870).

Configuration	X(cm)	Y(cm)	Z(cm)
1)Mono, 1 marker	0.4	0.15	0.9
2)Stereo, 1 marker	0.4	0.15	0.8
3)Mono, 2 markers	0.4	0.20	1.1

Table 2: Peak to peak errors

10. REFERENCES

[1] M. Born and E. Wolf, “Principles of optics”, Pergamon Press, 1964.

[2] C. Bruschini and B. Gros, “A Survey of Current Sensor Technology Research for the Detection of Landmines”, *International Workshop on Sustainable Humanitarian Demining (SusDem’97)*, 29 september-1 October 1997, Zagreb, Croatia.

[3] J. A. Craib, “Mine detection and demining from an operator’s perspective”, *Workshop of antipersonnel mine detection and removal*, Lausanne, 30^{th} June and 1^{st} July 1995.

[4] S. Havlík and P. Licko, “Humanitarian demining: the challenge for robotic research”, *Journal of Humanitarian demining*, Issue 2.2, June 1998.

[5] HOPE, “Hand-held OPErational demining system (HOPE)”, Esprit Project 29870, DG III.

[6] N. Milisavljevic, “Comparison of three methods for shape recognition in the case of mine detection”, *Pattern Recognition Letters*, vol. 20, issue 11-13, pp. 1079-1083, 1999.

[7] N. Milisavljevic, B. Scheers, O. Thonnard, M. Acheroy, “3D visualization of data acquired by laboratory UWB GPR in the scope of mine detection”, In *Proceedings of EUROCONFERENCE ON: Sensor systems and signal processing techniques applied to the detection of mines and unexploded ordnance (Mine’99)*, Florence, Italy, 1999.

[8] I. Popova, “Gyrostabiliser for Mobile Antenna Post”, PhD thesis, Technische Universiteit Delft, The Netherlands, 1996.

[9] O. Thonnard and N. Milisavljevic, “Metallic shape detection and recognition with a metal detector”, In *Proceedings of the European Workshop on Photonics applied to Mechanics and Environmental Testing Engineering (PHOTOMEC’99 - ETE’99)*, Liège, Belgium, 1999.

[10] R. Y. Tsai, “An efficient and accurate camera calibration technique for 3D machine vision”, In *Computer Vision and Pattern Recognition*, Miami, 1986.